Nonisothermal Melt Crystallization Kinetics of Poly(Ethylene Terephthalate)/Clay Nanocomposites

Yaming Wang, Changyu Shen, Haimei Li, Qian Li, Jingbo Chen

National Engineering Research Center for Advanced Polymer Processing Technology, Zhengzhou University, Zhengzhou 450002, China

Received 19 September 2002; accepted 23 April 2003

ABSTRACT: Various kinetic models, namely, the Avrami analysis modified by Jeziorny, the Ozawa model, and a method developed by Mo, were applied to describe the nonisothermal melt crystallization process of poly(ethylene terephthalate) (PET) and two PET/clay nanocomposites of different viscosities. The Avrami analysis modified by Jeziorny could gratifyingly describe the primary nonisothermal crystallization stage of PET and two PET/clay nanocomposites. The difference in the values of the Avrami exponent between PET and PET/clay nanocomposites suggested that the nonisothermal crystallization of PET/clay nanocomposites corresponds to a tridimensional growth with heterogeneous nucleation. The values of half-time showed that the crystallization rate of PET/clay nanocomposites is faster than that of PET at a given cooling rate. The Ozawa analysis failed to provide an adequate description of the nonisothermal crystallization of PET/clay nanocomposites. The method developed by Mo was successful in describing the nonisothermal crystallization of pristine PET and PET/clay nanocomposites. The activation energy for nonisothermal crystallization of pristine PET and two PET/clay nanocomposites of different viscosities, based on the Augis–Bennett method, the Kissinger method, and the Takhor method, respectively, were evaluated, and it was concluded that the absolute value of activation energy for PET is lower than that of PET/clay nanocomposites, and this showed that introduction of clay into PET matrix weakens the dependence of the nonisothermal crystallization exotherms peak temperatures on the cooling rates used. © 2003 Wiley Periodicals, Inc. J Appl Polym Sci 91: 308–314, 2004

Key words: polyesters; clay; nanocomposites; crystallization; kinetics

INTRODUCTION

Poly(ethylene terephthalate) (PET) is a slow crystallizing polymer, despite its important industrial applications. To accommodate typical industrial injection molding processes, additives (most often nucleating agents) are introduced to increase the rate of PET crystallization. Inorganic compounds, such as $CaCO_3$, and fiber have been found to enhance crystallization by dense heterogeneous nucleation on the surface of additive particles.[1,2] Recently, a new class of materials, PET/clay nanocomposites, has been developed successfully.[3,4] Dispersion of the inorganic filler at the nanometer scale has led to significant improvements in the properties of such nanocomposites, which has unique properties that are not shared by conventional composites, such as high strength, high modulus, and high heat distortion temperature.

Up to now, the studies on PET/clay nanocomposites[3,4] are mainly focused on its synthesis, nanoscale morphology, and crystallization behavior. An understanding of dynamic crystallization behavior is of great importance, because most processing techniques actually occur under nonisothermal conditions. In addition, nonisothermal crystallization can broaden and supplement the knowledge of the crystallization behavior of polymers.

In this article, the nonisothermal crystallization behavior of pristine PET and PET/clay nanocomposites was studied by a differential scanning calorimeter (DSC). Different theoretical approaches[5–8] were used to describe the kinetics of nonisothermal crystallization. The activation energy describing the nonisothermal crystallization process was also calculated on the basis of various theories.[9–11]

EXPERIMENTAL

Materials and sample preparation

The pristine PET and PET/clay nanocomposites pellets used in this study were kindly supplied in pellet form by Yanshan Petrochemical Co., Ltd. (Beijing, China). The intrinsic viscosities of the pellets measured in 50/50 (w/w) of 1,1,2,2-tetrachloroethane/phenol, at 25°C, 0.1 g/100 mL concentration, are 0.65 for pristine PET, 0.61 for PET/clay no. 1 nanocomposite (with clay weight content of 1.5%), and 0.82 for PET/clay no. 2

Correspondence to: Y. Wang (wangyaming@zzu.edu.cn).
Contract grant sponsor: Young Standout Teacher Funds of Universities (Henan Province, China).

Journal of Applied Polymer Science, Vol. 91, 308–314 (2004)

nanocomposite (with clay weight content of 1.5%), respectively. Sample films of ~ 0.2 mm were obtained by hot-press at 280°C for several minutes.

DSC measurements

In this article, a TA 2920 DSC was used to study the kinetics of crystallization. Temperature calibration was performed by using an indium standard. Sample weight varied between 5.2 and 5.5 mg, which was cut from the film.

The experiment started with heating the sample from room temperature to 280°C, where it was held for 10 min to eliminate small residual nuclei that might act as seed crystals. Then, the melt was cooled to crystallize at selected constant cooling rates ϕ, ranging from 2.5 to 20°C/min. It is noteworthy that each sample was used only once and all the runs were carried out under a nitrogen purge.

RESULTS AND DISCUSSION

Nonisothermal crystallization behavior

The crystallization exotherms of pristine PET and PET/clay nanocomposites for nonisothermal crystallization from the melt at four different cooling rates ranging from 2.5 to 20°C/min are presented in Figure 1. Clearly, the exothermic curve becomes wider and shifts to the lower temperature region as the cooling rate increases; these are apparently true for all of the PET and PET/clay nanocomposites samples studied in this article. The values of the nonisothermal crystallization exotherms peak temperatures, T_p, and the crystallization enthalpies, ΔH_c, of all the samples under different cooling rates are collected in Table I. It can be seen that, for a given cooling rate, the PET/clay no. 1 nanocomposite's $T_p >$ PET/clay no. 2 nanocomposite's $T_p >$ PET's T_p. This means that the clay in PET is a nucleating agent, and therefore, increases the crystallization rate of PET. For the nonisothermal crystallization of PET and both PET/clay no. 1 and PET/clay no. 2 nanocomposites, ΔH_c are all increasing as the cooling rate decreases. Because the absolute degree of crystallization of sample is equal to the enthalpy for unit mass of sample, ΔH_c, divided by the heat of fusion of a perfect PET crystal, it can be concluded from Table I that the absolute degree of PET/clay nanocomposites is lower than that of pure PET.

The relative degree of crystallinity $X(T)$, as a function of crystallization temperature T, can be formulated as[12]

$$X(T) = \int_{T_0}^{T} \left(\frac{dH_c}{dT}\right) dT \Big/ \int_{T_0}^{T_\infty} \left(\frac{dH_c}{dT}\right) dT \qquad (1)$$

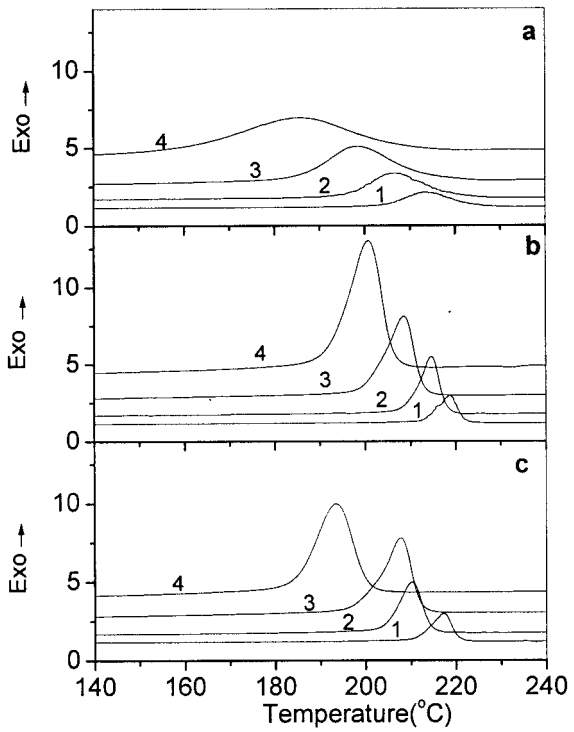

Figure 1 Nonisothermal melt crystallization exotherms of (a) PET, (b) PET/clay no. 1 nanocomposite, and (c) PET/clay no. 2 nanocomposite at four different cooling rates: 1, 2.5°C/min; 2, 5°C/min; 3, 10°C/min; 4, 20°C/min.

where T_0 and T_∞ represent the crystallization onset and end temperature, respectively, and dH_c is the enthalpy of crystallization released during an infinitesimal temperature range dT.

Figure 2 shows the relative degree of crystallinity as a function of temperature for PET and PET/clay nanocomposites at various cooling rates. The horizontal temperature scale, such as shown in Figure 2, can be transformed into time domain by using the relationship

$$t = (T_0 - T)/\phi \qquad (2)$$

where T is the temperature at crystallization time t, and ϕ is the cooling rate. The plots of the relative degree of crystallinity as a function of time for PET and PET/clay nanocomposites at different cooling rates are illustrated in Figure 3.

An important parameter which can be taken directly from Figure 3 is the half-time of crystallization $t_{1/2}$, which is the change in time from the onset of crystallization to the time at which $X(t)$ is 50%. The $t_{1/2}$ of nonisothermal crystallization for PET and PET/clay nanocomposites are listed in Table I. It can be seen that the higher the cooling rate, the shorter the time for completing the crystallization. For a given cooling rate, as expected, the PET/clay no. 1 nanocomposite's

TABLE I
Characteristic Data of Nonisothermal Crystallization Exotherms for Various Samples

Sample	Intrinsic viscosity	ϕ (°C/min)	T_p (°C)	$t_{1/2}$ (min)	ΔH_c (J/g)
PET	0.65	2.5	213.29	9.63	54.89
		5	206.74	5.34	54.36
		10	198.57	2.73	47.55
		20	185.53	1.86	38.63
PET/clay no. 1 nanocomposite	0.61	2.5	218.63	4.23	49.96
		5	214.65	1.80	49.23
		10	208.54	1.31	47.30
		20	200.74	0.76	44.24
PET/clay no. 2 nanocomposite	0.82	2.5	217.07	5.14	49.33
		5	210.22	2.83	48.55
		10	207.74	1.38	46.01
		20	193.50	1.06	34.56

$t_{1/2}$ < PET/clay no. 2 nanocomposite's $t_{1/2}$ < PET's $t_{1/2}$. This can further demonstrate that the clay plays a nucleating role.

Nonisothermal crystallization kinetics based on Avrami equation modified by Jeziorny

The most common approach used to analyze the isothermal crystallization kinetics is the Avrami equation,[5] which assumed that the relative crystallinity $X(t)$developed with crystallization time t,

$$1 - X(t) = \exp(-Zt^n) \tag{3}$$

where Z is the composite crystallization rate constant, and n is the Avrami exponent. It should be mentioned that in nonisothermal crystallization, the Z and n parameters do not have the same physical meaning as in the isothermal crystallization because the temperature changes instantly in the nonisothermal crystallization.

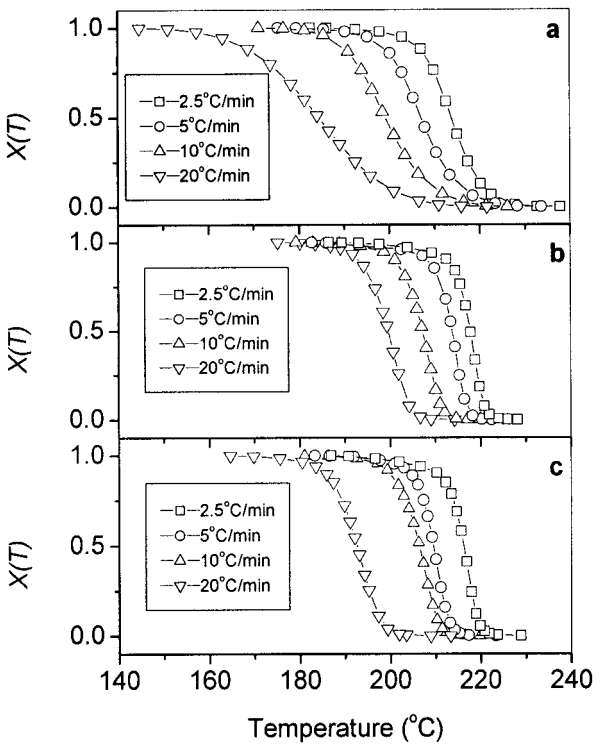

Figure 2 $X(T)$ as a function of temperature for crystallization of (a) PET, (b) PET/clay no. 1 nanocomposite, and (c) PET/clay no. 2 nanocomposite at four different cooling rates.

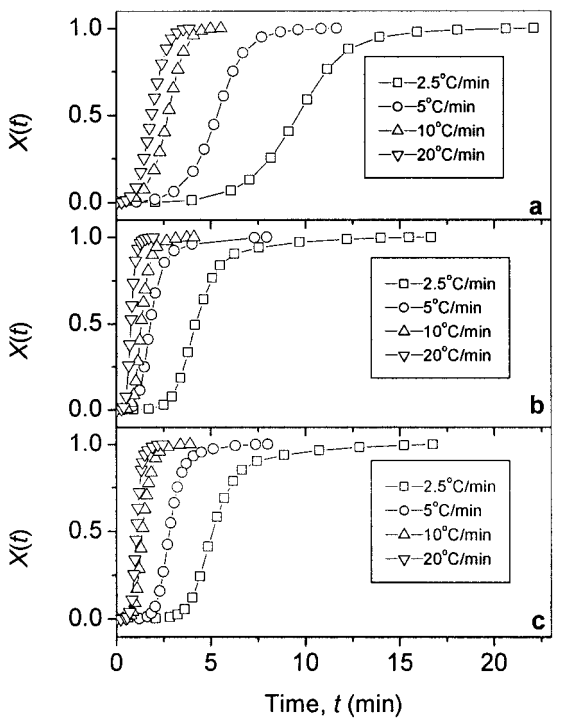

Figure 3 $X(t)$ as a function of time for crystallization of (a) PET, (b) PET/clay no. 1 nanocomposite, and (c) PET/clay no. 2 nanocomposite at four different cooling rates.

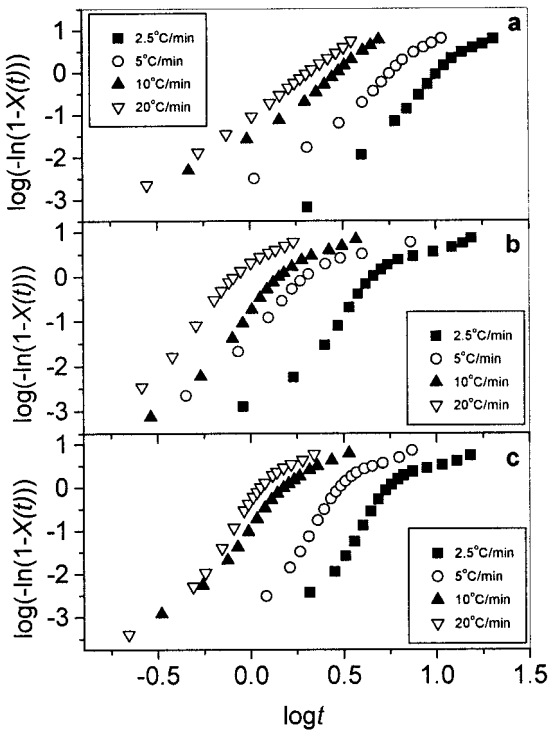

Figure 4 Plots of $\log[-\ln(1 - X(t))]$ versus $\log t$ for crystallization of (a) PET, (b) PET/clay no. 1 nanocomposite, and (c) PET/clay no. 2 nanocomposite at four different cooling rates.

In this case, Z and n are two adjustable parameters to be fit to the data. However, the use of eq. (3) can still provide further insight into the kinetics of nonisothermal crystallization.

Considering the nonisothermal character of the process investigated, Jeziorny[6] suggested that the value of rate parameter Z should be adequately corrected. The factor that should be considered was the cooling rate, ϕ. Assuming constant or approximately constant ϕ, the final form of the parameter characterizing the kinetics of nonisothermal crystallization was given as:

$$\log Z_c = (\log Z)/\phi \quad (4)$$

Figure 4 shows the double logarithmic plots of $\log[-\ln(1 - X(t))]$ versus $\log t$ for PET and PET/clay nanocomposites at various cooling rates. Each curve has a linear portion, most of which is followed by a gentle deviation at longer times. Usually, this deviation is considered to be due to the secondary crystallization, which is caused by the spherulite impingement in the later stage. The linear portions are almost parallel to each other, shifting to a shorter time with increasing ϕ, indicating that the nucleation mechanism and crystal growth geometries are similar for the primary and secondary crystallization at all cooling rates. Each region gives different values for n (n_1 and n_2) and Z_c (Z_{c1} and Z_{c2}) (Table II). For the nonisothermal melt crystallization of PET, n_1 varies from 3.23 to 4.74, and n_2 varies from 1.81 to 2.18; for PET/clay no. 1 nanocomposite, n_1 varies from 4.21 to 5.98, and n_2 varies from 1.16 to 2.00; for PET/clay no. 2 nanocomposite, n_1 varies from 5.71 to 7.11, and n_2 varies from 1.18 to 1.97. There was some confusion of Avrami exponent values of pristine PET in the literature, which is attributed to the complication of PET crystallization. For example, Jeziorny[6] found Avrami exponent values of pristine PET equal to 2.3, 2.5, and 2.6 for cooling rates of 8.5, 12, and 17°C/min, respectively. The values ranging from 2.5 to 2.9 were instead obtained by Duillard and coworkers[13] in the temperature range of 220–235°C. Obviously, the average values of n_1 for both PET/clay no. 1 and PET/clay no. 2 nanocomposites are larger than that of pristine PET, suggesting that the nonisothermal crystallization of PET/clay nanocomposites corresponds to a tridimensional growth with heterogeneous nucleation. The same conclusion is reasonable for PET[2] and for polypropylene (PP)[14] with nucleating agents in isothermal crystallization, and for poly(oxymethylene)/montmorillonite (POM/MMT) nanocomposite in nonisothermal crystallization.[15] The Z_c values of both PET/clay no. 1 and PET/clay no. 2 nanocomposites are higher than that of pristine PET at the same cooling rate.

Nonisothermal crystallization kinetics based on Ozawa approach

Based on the mathematical derivation of Evans, Ozawa[7]extended the Avrami theory to be able to describe the nonisothermal case. Mathematically, the relative crystallinity can be written as a function of cooling rate according to the equation

TABLE II
Nonisothermal Crystallization Kinetic Parameters Based on Avrami Equation Modified by Jeziorny

		Primary stage		Secondary stage	
Sample	ϕ (°C/min)	n_1	Z_{c1}	n_2	Z_{c2}
PET	2.5	4.74	0.012	1.81	0.228
	5	4.40	0.213	2.18	0.512
	10	3.72	0.663	—	—
	20	3.23	0.887	—	—
PET/clay no. 1 nanocomposite	2.5	5.98	0.028	1.16	0.592
	5	4.21	0.556	1.02	0.952
	10	5.47	0.832	1.54	0.986
	20	5.07	1.059	2.00	1.037
PET/clay no. 2 nanocomposite	2.5	7.11	0.008	1.18	0.536
	5	6.85	0.223	1.68	0.751
	10	5.71	0.803	1.79	0.964
	20	6.56	0.963	1.97	1.011

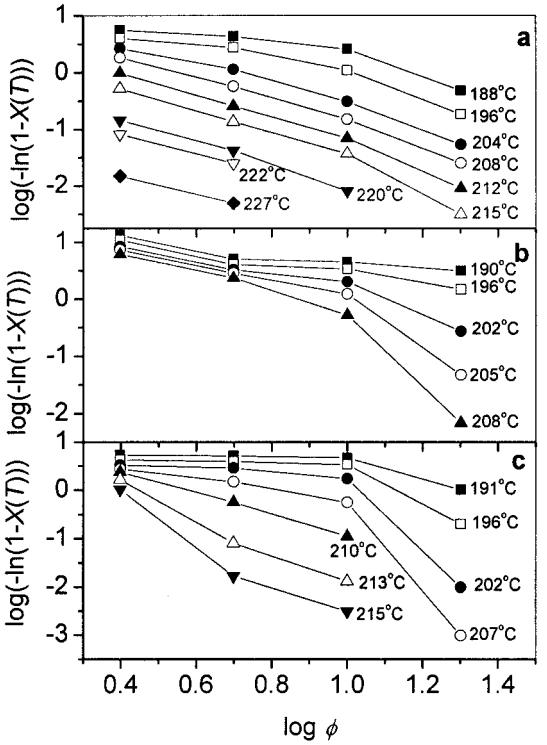

Figure 5 Ozawa plots of $\log[-\ln(1 - X(T))]$ versus $\log \phi$ for crystallization of (a) PET, (b) PET/clay no. 1 nanocomposite, and (c) PET/clay no. 2 nanocomposite.

$$1 - X(T) = \exp[-K(T)/\phi^m] \tag{5}$$

where $K(T)$ is the Ozawa crystallization rate constant, and m is the Ozawa exponent (which is similar to the Avrami exponent). Taking the double-logarithmic form,

$$\log[-\ln(1 - X(T))] = \log K(T) - m \log \phi \tag{6}$$

and plotting $\log[-\ln(1 - X(T))]$ against $\log \phi$ at a given temperature, a straight line should be obtained if the Ozawa method is valid. The Ozawa crystallization rate constant $K(T)$ is taken as the antilogarithmic value of the y-intercept, and the Ozawa exponent m is taken as the negative value of the slope. Figure 5 illustrates such plots based on the nonisothermal crystallization data of PET and PET/clay nanocomposites for a series of temperatures. It can be seen that, for PET, the plot of $\log[-\ln(1 - X(T))]$ against $\log \phi$ results in a series of parallel lines at relatively higher temperatures, and parts of the Ozawa exponents are 1.89, 2.05, 2.22, 2.4, and 2.08 at 204, 208, 212, 215, and 220°C, respectively. It is fair to conclude that the Ozawa approach can well describe the nonisothermal crystallization kinetics at least at relatively higher temperatures, although the Ozawa exponents obtained here are lower than that reported by Ozawa.[7] The cooling rates used by Ozawa[7] for the analysis of PET kinetics were 1, 2, and 4°C/min, and the Ozawa exponents, calculated by using the Ozawa equation, were 3.4, 3.6, and 3.6 at 220, 222, and 227°C, respectively. However, Figure 5 shows some nonparallel lines for PET at the lower temperature regions, and for both PET/clay no. 1 and PET/clay no. 2 nanocomposites, which is similar to that observed in poly(ether-ether ketone) (PEEK),[16] poly(ether ketone ether ketone ketone) (PEKEKK),[17] and POM/MMT nanocomposites.[15] It is important to note that Ozawa equation ignored secondary crystallization.[7] In fact, from Figure 4, it can be seen that most curves, except for that of PET at the cooling rates of 20 and 10°C/min, have a gentle deviation at longer times. Therefore, the reason that the nonisothermal crystallization of PET at the lower temperature regions, and both PET/clay no. 1 and PET/clay no. 2 nanocomposites, does not follow the Ozawa equation can be explained that, at a given temperature, the crystallization processes at different cooling rates are at different stages, that is, the lower cooling rate process is toward the end of the crystallization process, whereas at the higher cooling rate, the crystallization process is at an early stage.

Nonisothermal crystallization kinetics combined Avrami equation and Ozawa equation

A method developed by Mo[8] was also employed to describe the nonisothermal crystallization for comparison. For the nonisothermal crystallization process, physical variables relating to the process are the relative degree of crystallinity $X(t)$, cooling rate ϕ, and crystallization temperature T. Both the Ozawa and the Avrami equations can relate these variables as

$$\log Z + n \log t = \log K(T) - m \log \phi \tag{7}$$

and by rearrangement, its final form is given as

$$\log \phi = \log F(T) - a \log t \tag{8}$$

where the kinetic parameter $F(T) = [K(T)/Z]^{1/m}$ refers to the value of cooling rate that has to be chosen at the unit crystallization time when the measured system amounts to a certain degree of crystallinity; a is the ratio of the Avrami exponent n to the Ozawa exponent m (i.e., $a = n/m$). At a given degree of crystallinity, by plotting $\log \phi$ versus $\log t$ (Fig. 6), the values of a and $F(T)$ could be obtained by slopes and intercepts of these lines, respectively (Table III). The values of $F(T)$ systematically increase with an increase in the relative crystallinity for pristine PET and two PET/clay nanocomposites, which means, at unit crystallization time, a higher cooling rate should be used to obtain a higher degree of crystallinity, although the values of a are almost constant for each sample, which vary from 1.16 to 1.26 for PET, from 1.20 to 1.23 for PET/clay no. 1

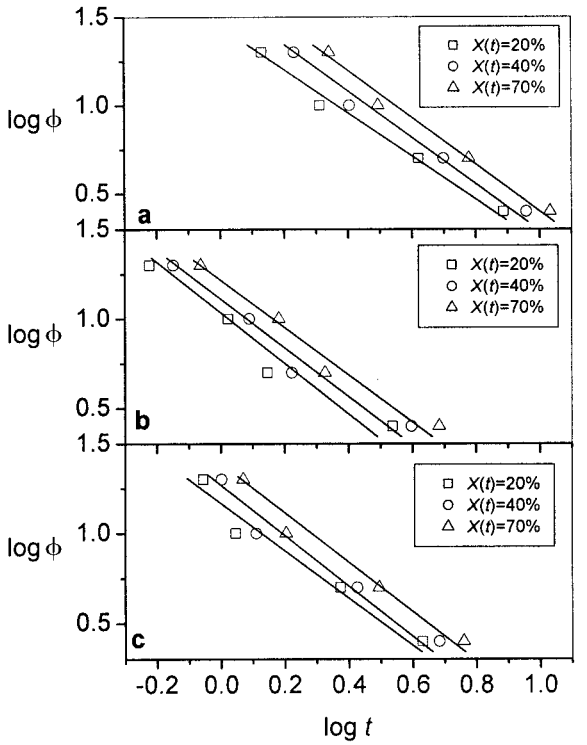

Figure 6 Plots of log ϕ versus log t for (a) PET, (b) PET/clay no. 1 nanocomposite, and (c) PET/clay no. 2 nanocomposite.

nanocomposite, and from 1.22 to 1.25 for PET/clay no. 2 nanocomposite. It is clear that this combination method is successful in describing the nonisothermal process of pristine PET and two PET/clay nanocomposites, which is also true for PEEK,[16] PEKEKK,[17] and POM/MMT nanocomposites.[15]

Activation energy describing the overall crystallization process

The activation energy ΔE of nonisothermal crystallization can be evaluated from methods such as those proposed by Augis and Bennett,[9] Kissinger,[10] or Takhor.[11] Considering the variation of the peak temperature T_p with the cooling rate ϕ (cf. Table I), the activation energy ΔE can be evaluated based on plots of the following forms: (1) Augis–Bennett method,

$$\frac{d[\ln(\phi/(T_0 - T_p))]}{d(1/T_p)} = -\frac{\Delta E}{R} \tag{9}$$

where T_0 is an initial temperature ($\sim$ 279°C for PET and PET/clay nanocomposites), and R is the universal gas constant; (2) Kissinger method,

$$\frac{d[\ln(\phi/T_p^2)]}{d(1/T_p)} = -\frac{\Delta E}{R} \tag{10}$$

and (3) Takhor method,

$$\frac{d[\ln(\phi)]}{d(1/T_p)} = -\frac{\Delta E}{R} \tag{11}$$

Figure 7 illustrates plots based on the Augis–Bennett method, the Kissinger method, and the Takhor method, respectively (data from Table I). The slopes of the least-square lines drawn through these plots equal $-\Delta E/R$; thus, the activation energy ΔE can be calculated accordingly. The results of ΔE are collected in Table IV. It can be concluded that the absolute value of

TABLE III
Nonisothermal Crystallization Kinetic Parameters of Various Samples at Different Degrees of Crystallinities by Combination of Avrami–Ozawa Equation

$X(t)$ (%)	20	40	70
	PET		
$F(T)$	25.92	34.76	48.24
a	1.16	1.20	1.26
	PET/clay no. 1 nanocomposite		
$F(T)$	9.87	12.09	15.73
a	1.20	1.22	1.23
	PET/clay no. 2 nanocomposite		
$F(T)$	14.19	16.84	21.18
a	1.22	1.23	1.25

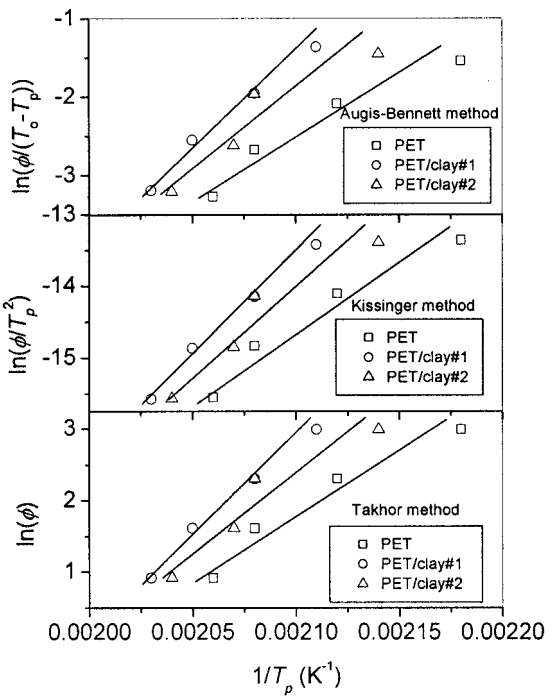

Figure 7 Determination of the activation energy ΔE describing the nonisothermal crystallization process for PET and PET/clay nanocomposites based on various theoretical methods.

TABLE IV
Activation Energy ΔE Describing the Overall Crystallization Process of Various Samples

Sample	Activation energy ΔE (kJ mol^{-1})		
	Augis–Bennett	Kissinger	Takhor
PET	−113.5	−144.8	−136.8
PET/clay no. 1 nanocomposite	−192.3	−227.6	−219.4
PET/clay no. 2 nanocomposite	−136.8	−170.5	−162.4

ΔE for PET is lower than that of two PET/clay nanocomposites of different viscosities, which is true for all three methods mentioned above. Apparently, this should conclude that PET/clay nanocomposites crystallizes slower than PET; however, this is in contradiction with the main conclusion obtained from the results of crystallization kinetics above. Therefore, the values of ΔE evaluated from the above methods are just adjustable parameters and do not possess the same physical meaning as the activation energy, generally speaking. Nevertheless, the values of ΔE evaluated from the above methods can give a finite relationship between the peak temperature T_p obtained from the nonisothermal crystallization exotherms and the cooling rates ϕ used. It can be concluded from the above results that introduction of clay into PET matrix weakens the dependence of the nonisothermal crystallization exotherms peak temperatures T_p on the cooling rates ϕ used.

CONCLUSION

The nonisothermal melt crystallization data of pristine PET and two PET/clay nanocomposites of different viscosities studied by using DSC were analyzed according to three different kinetics models, namely, the Avrami analysis modified by Jeziorny, the Ozawa model, and a method developed by Mo. The Avrami analysis modified by Jeziorny could gratifyingly describe the primary nonisothermal crystallization stage of PET and two PET/clay nanocomposites, and the deviation of linearity at the longer time might be ascribed to the occurrence of the spherulite impingement in the secondary stage. The difference in the values of the Avrami exponent n_1 between pristine PET and PET/clay nanocomposites suggested that the nonisothermal crystallization of PET/clay nanocomposites corresponds to a tridimensional growth with heterogeneous nucleation. The values of half-time showed that the crystallization rate of PET/clay nanocomposites is faster than that of PET at a given cooling rate. The Ozawa analysis failed to provide an adequate description of the nonisothermal crystallization of PET/clay nanocomposites; this might be due to secondary crystallization. The method developed by Mo was successful in describing the nonisothermal crystallization of pristine PET and PET/clay nanocomposites. Last, the activation energy for nonisothermal crystallization of pristine PET and two PET/clay nanocomposites of different viscosities, based on the Augis–Bennett method, the Kissinger method, and the Takhor method, respectively, were evaluated, and a consistent conclusion was made that the absolute value of ΔE for PET is lower than that of two PET/clay nanocomposites of different viscosities. This showed that introduction of clay into PET matrix weakens the dependence of the nonisothermal crystallization exotherms peak temperatures T_p on the cooling rates ϕ used.

The authors gratefully acknowledge the financial support from the Young Standout Teacher Funds of Universities in Henan Province, China.

References

1. Zhu, P.; Ma, D. Eur Polym J 2000, 36, 2471.
2. Reinsch, V. E.; Rebenfeld, L. J Appl Polym Sci 1994, 52, 649.
3. Ke, Y.; Long, C.; Qi, Z. J Appl Polym Sci 1999, 71, 1139.
4. Ke, Y.; Yang, Z.; Zhu, C. J Appl Polym Sci 2002, 85, 2677. *0*
5. Avrami, M. J Chem Phys 1940, 8, 212.
6. Jeziorny, A. Polymer 1978, 19, 1142.
7. Ozawa, T. Polymer 1971, 12, 150.
8. Liu, T. X.; Mo, Z. S.; Wang, S. E.; Zhang, H. F. Polym Eng Sci 1997, 37, 443.
9. Augis, J. A.; Bennett, J. E. J Thermal Anal 1978, 13, 283.
10. Kissinger, H. E. J Res Natl Bur Stand 1956, 57, 217.
11. Takhor, R. L. Advances in Nucleation and Crystallization of Glasses; American Ceramics Society: Columbus, OH, 1971; pp 166–172.
12. Cebe, P.; Hong, S.-D. Polymer 1986, 27, 1183.
13. Duillard, A.; Dumazed, P.; Chabert, B.; Guillet, J. Polymer 1993, 34, 1702.
14. Lim, G. B. A.; Lloyd, D. R. Polym Eng Sci 1993, 33, 513.
15. Xu, W.; Ge, M.; He, P. J Appl Polym Sci 2001, 82, 2281.
16. Liu, T. X.; Mo, Z. S.; Wang, S. E.; Zhang, H. F. Polym Eng Sci 1997, 37, 568.
17. Qiu, Z.; Mo, Z.; Yu, Y.; Zhang, H.; Sheng, S.; Song, C. J Appl Polym Sci 2000, 77, 2865.